Radiative Heat Transfer during Turbulent Combustion Process

S. C. Paul and M. C. Paul *
Department of Mechanical Engineering, University of Glasgow,
Glasgow G12 8QQ, UK

Abstract

We investigate the radiative heat transfer in a co-flowing turbulent non-premixed propane-air flame inside a three-dimensional cylindrical combustion chamber. The radiation from the luminous flame, which is due to the appearance of soot particles in the flame, is studied here, through the balance equation of radiative transfer which is solved by the Discrete Ordinates Method (DOM) coupling with a Large Eddy Simulation (LES) of the flow, temperature, combustion species and soot formation. The effect of scattering is ignored as it is found that the absorption dominates the radiating medium. Assessments of the various orders of DOM are also made and we find that the results of the incident radiation predicted by the higher order approximations of the DOM are in good agreement.

Keywords: Discrete Ordinates Method, Large Eddy Simulation, Radiative Heat Transfer, Turbulent Combustion

*E-mail:m.paul@mech.gla.ac.uk, Tel:+44 (0)141 330 8466, Fax:+44 (0)141 330 4343

Nomenclature

Roman Characters

f	mixture fraction
f_v	soot volume fraction
G	incident radiation
I	radiative intensity
J_j	SGS mixture fraction fluxes
M	total number of the discrete directions
p	dynamic pressure
q	radiative heat fluxes
Q	efficiency factor
Sc	Schmidt number
t	time
T	temperature
u_j	velocity components
x_j	Cartesian coordinates, (x, y, z)
Y_α	mole fraction of species α
$Y_{c(s)}$	soot mass fraction

Greek Symbols

α, β, γ	direction cosines
δ	Kronecker delta
κ	absorption coefficient
μ	coefficient of viscosity
ϕ	soot mass fraction/particle number density
Φ_j	SGS fluxes of ϕ
ρ	fluid density
$\rho_{c(s)}$	soot density
σ	Stefan-Boltzmann constant
τ_{ij}	SGS stresses
ε	emissivity

Subscripts

abs	absorption
b	black body
m	angular discrete direction
n	order of S_n approximation
sca	scattering
w	wall

Mathematical Accents

$\bar{.}$	spatial filtered quantities
$\tilde{.}$	Favre filtered quantities

Abbreviations

DOM Discrete Ordinates Method
LES Large Eddy Simulation
RTE Radiative Transfer Equation
SGS Sub Grid Scale

1 Introduction

In most combustion devices such as furnaces, gas turbines, internal combustions engines, burners, etc., a large portion of the total heat flux/transfer occurs mainly by radiation from the flame. In a fuel-rich combustion, the ratio of fuel to air is high and mixing of fuel with air is inadequate, which lead to the production of solid soot particles. The radiation occurs in both non-luminous and luminous flames. The radiation emitted from non-luminous flame depends on the hot combustion products, mainly carbon dioxide (CO_2) and water vapour (H_2O). On the other hand, the luminous radiation is mainly for the appearance of soot particles in the flame. For an efficient design of a combustion system with less pollutant emissions, it is essential to predict the wall temperature accurately which in turn depends on the accurate prediction of the radiative heat transfer. Therefore, an adequate treatment of thermal radiation is essential to develop a mathematical model for the combustion processes.

To predict the radiative heat transfer in high temperature combustion process, it requires a simultaneous solution of the RTE and the governing equations of flow which usually include the Navier-Stokes equations, the mixture fraction equation, etc, see [1; 2; 3]. A very few number of works has been done to date that involves the combination of DOM with LES to solve the radiative heat transfer in a turbulent flame, see the two-dimensional work of Desjardin and Frankel [2] who studied a strongly radiating nonpremixed turbulent jet flame, and the most recent work of Jones and Paul [3] and Paul [4] who investigated non-luminous flame radiation in a three-dimensional gas turbine combustor. It should be noted here that the Discrete Ordinates Method (DOM), Chandrasekhar [5] and Carlson and Lathrop [6], has become a popular method for solving the RTE because it shares computational grid with the finite volume approach, however, combining with LES for turbulent flame radiation is a challenging task.

A schematic of the cylindrical combustor with computational domain is shown in Fig. 1, for the experimental details see Nishida and Mukohara [7]. Gaseous propane (C_3H_8) is injected through the circular nozzle of an internal diameter of $2mm$ at the centre of the combustor inlet while the preheated air with an averaged velocity of $0.96ms^{-1}$ and temperature of $773K$ is supplied through the circular inlet of $115mm$ internal diameter into the $350mm$ long combustion chamber. The overall equivalence ratio is kept at 1.67 so that burning occurs in a fuel-rich nonpremixed combustion mode. The average fuel velocity measured by [7] at the inlet was $30ms^{-1}$, which corresponds to a flow Reynolds number of $13,000$ in the computation. To the best of authors' knowledge, this is the first time that a detailed investigation on the radiative transfer from the propane-air turbulent flame inside this combustion chamber is performed by combining DOM with LES.

2 Governing equations

The equations of motion in LES are obtained after applying a spatial filter [8] and a density weighted Favre filter [9] to the continuity, the Navier-Stokes, the mixture fraction, the soot mass fraction and the soot particle umber density equations. In DOM the discrete ordinates representation of the radiative transfer equation is filtered using the same spatial filter. Finally these equations take the following forms:

$$\frac{\partial \bar{\rho}}{\partial t} + \frac{\partial \bar{\rho}\tilde{u}_j}{\partial x_j} = 0 \,, \tag{1}$$

$$\frac{\partial \bar{\rho}\tilde{u}_i}{\partial t} + \frac{\partial \bar{\rho}\tilde{u}_i\tilde{u}_j}{\partial x_j} = -\frac{\partial \bar{p}}{\partial x_i} + \frac{\partial}{\partial x_j}\left(2\mu\bar{S}_{ij} - \frac{2}{3}\mu\bar{S}_{kk}\delta_{ij}\right) - \frac{\partial \tau_{ij}}{\partial x_j} \,, \tag{2}$$

$$\frac{\partial \bar{\rho}\tilde{f}}{\partial t} + \frac{\partial \bar{\rho}\tilde{u}_j\tilde{f}}{\partial x_j} = \frac{\partial}{\partial x_j}\left(\Gamma\frac{\partial \bar{f}}{\partial x_j}\right) - \frac{\partial J_j}{\partial x_j} \,, \tag{3}$$

$$\frac{\partial (\bar{\rho}\tilde{\phi})}{\partial t} + \frac{\partial (\bar{\rho}\tilde{u_j\phi})}{\partial x_j} = \frac{\partial}{\partial x_j}\left(\Gamma\frac{\partial \tilde{\phi}}{\partial x_j}\right) + \bar{\rho}\tilde{S}(\tilde{\phi}) - \frac{\partial \Phi_j}{\partial x_j} \,, \tag{4}$$

$$\alpha_m\frac{\partial \bar{I}_m}{\partial x} + \beta_m\frac{\partial \bar{I}_m}{\partial y} + \gamma_m\frac{\partial \bar{I}_m}{\partial z} + \overline{\kappa I_m} = \overline{\kappa I_b} \,. \tag{5}$$

where ρ is the mixture density, t is the time, $x_j = (x, y, z)$ is the coordinate vector, u_j is the velocity vector, p is the dynamic pressure, μ is the coefficient of viscosity, S_{ij} is the strain rate defined as $S_{ij} = \frac{1}{2}\left(\frac{\partial u_i}{\partial x_j} + \frac{\partial u_j}{\partial x_i}\right)$, δ_{ij} is the Kronecker delta, f is the mixture function, $\Gamma = \frac{\mu}{Sc}$ is the diffusion coefficient where Sc is the Schmidt number, and ϕ represents the soot mass fraction and the soot particle number density. In addition, some details about the source terms, $\bar{\rho}\tilde{S}(\tilde{\phi})$, in eqn (4), can be found in Paul *et al.* [10].

In eqn (5), I_m represents the radiative intensity along the angular direction, where $m = 1, 2, ..., M$ (see [11; 3] for a detailed angular representation), thus this equation represents a set of M different directional radiative intensities from a computational grid node. The terms α_m, β_m and γ_m in eqn (5) represent the direction cosines of an angular direction along the coordinates and I_b is the blackbody intensity at the temperature of the medium which is defined as $\frac{\sigma\tilde{T}^4}{\pi}$ where σ is the Stefan-Boltzmann constant and $\tilde{T}$ is the flame temperature. κ is the absorption coefficient, and for a luminous flame radiation, which is considered in this work, it is calculated as a sum of the mixture of CO_2 and H_2O with the soots as

$$\bar{\kappa} = 0.1\left(\tilde{Y}_{CO_2} + \tilde{Y}_{H_2O}\right) + 1401.82\tilde{f}_v\tilde{T} \quad m^{-1} \,, \tag{6}$$

where $\tilde{Y}_{CO_2}$ and $\tilde{Y}_{H_2O}$ are the mole fractions of CO_2 and H_2O respectively, and $\tilde{f}_v$ is the soot volume fraction defined as $\tilde{f}_v = \frac{\bar{\rho}\tilde{Y}_{c(s)}}{\rho_{c(s)}}$ where $\tilde{Y}_{c(s)}$ represents the soot mass fraction and $\rho_{c(s)} = 2000kg/m^3$ is the soot density.

In eqns (2)-(4) the sub-grid scale stresses, τ_{ij}, and the sub-grid scale scalar fluxes, J_j and Φ_j, are modelled using the standard Smagorinsky model, [12], and a gradient model, [13], respectively. For the unknown terms, $\overline{\kappa I_m}$ and $\overline{\kappa I_b}$, in eqn (5), which are

the nonlinear correlations between turbulence and radiation, we have simply ignored the sub-grid scale turbulence interaction with radiation.

In the radiation modelling we have assumed that the enclosure contains an absorbing-emitting and radiatively gray medium. The effects of scattering in the modelling have been ignored, see Fig. 2, where the axial profiles of the scattering, Q_{sca}, and absorption, Q_{abs}, efficiency factors are presented. This figure shows that the order of absorption efficiency is of $O(10^{-2})$ while the scattering efficiency has an order of $O(10^{-6})$, which clearly suggests that the scattering in this flame can be neglected.

The detailed boundary conditions for solving the filtered eqns (1)-(4) are presented in Paul *et al.* [10], and while for the filtered RTE (5) the surfaces bounding the medium are considered to be diffusely emitting and reflective. In addition, the inlet and outlet boundaries are considered to be open and set to be black body absorption (Zheng *et al.* [14]), for which the radiation coming from the upstream of the inlet and downstream of the outlet do not affect the internal thermal field.

3 Numerical procedures

The filtered equations (1)-(5) are rewritten in general boundary/body fitted coordinates system using the approach introduced by Thompson [15], where the governing differential equations in the Cartesian coordinates are transformed into the curvilinear coordinates system. Some details of the numerical procedures in the LES to solve eqns (1)-(4) can be found in Paul *et al.* [10] and the relevant references therein, while the numerical procedures in DOM to solve the RTE (5) can be found in Jones and Paul [3]. Also a benchmark problem was considered in [3] to assess accuracy of the numerical results of the DOM in a general body fitted co-ordinates system, and a very good agreement was obtained compared with the results available in literature, for further details the readers are referred to [3].

4 Results and discussion

In the computation we employed a total of about 10^6 control volumes inside the combustion chamber and the results presented in Figs. 3 and 4 are at the timesteps of 3×10^5 which gives the real clock time of about $t \approx 0.743$ *sec.* A variable timestep was used in the computation to ensure that the maximum Courant number lies between 0.1 and 0.2 throughout the computations.

One of the important radiation quantities is the incident radiation, G, which is calculated using

$$\bar{G} = \int_{4\pi} \bar{I} d\Omega \approx \sum_{m=1}^{M} \omega_m \bar{I}_m \, , \tag{7}$$

and presented in Fig. 3 for the various orders of DOM (S_n) to show the effects of the different orders of approximation of DOM on G. The wall emissivity is taken as $\varepsilon_w = 0.5$ for all the approximations. In frame (a) the axial profiles on the centreline of the combustor are shown whereas the radial profiles at the two different cross-sectional positions are plotted in frames (b-c). It can be seen that

the incident radiation obtained by using the most lower order approximation, S_2, of the DOM diverges little bit from those with the higher orders. On the other hand the results of the higher order approximations (S_4, S_6 and S_8) converge together, proving the accuracy in the predictions of radiative transfer in the present model, which is very good despite the fact that no direct comparison with experimental data was possible to make because the radiation measurement was not performed by Nishida and Mukohara [7] in the flame.

In addition, the axial centreline profiles of G show that they increase towards the downstream of the combustor as the soot volume fraction as well as the flame temperature (see Fig. 4) increases. The peak values of G are predicted at the location where the peaks in the temperature and soot volume fraction are achieved. The incident radiations then decrease towards the outlet because of the slowly decrease in the temperature and soot volume fraction in this region. Moreover, the radial profiles of G show that the peak values which are predicted around the centre of the combustor, because of the high level of soot volume fraction and absorption coefficient in this region, decrease towards the combustor wall having minimum at the wall.

As mentioned, the incident radiation is an important radiation property related to the radiative energy density, by which the total radiation energy is stored in each computational node and which also allows us the radiative energy transfer to be coupled with the global energy conservation for the model. Therefore, the incident radiation results in Fig. 3 also represent a distinct variation of the radiative energy storage inside the combustion chamber.

In Fig. 4(a-d) contours of the instantaneous results of the flame temperature, mole fractions of CO_2 and H_2O, and soot volume fraction, $\tilde{f}_v$, are plotted respectively on the horizontal midplane of the combustor. Only the results obtained by S_6 are presented here, keeping the same value for the wall emissivity. The black body radiation, $\bar{I}_b$, is a function of both the flame temperature and the absorption coefficient, where the absorption coefficient for the luminous flame is again a function of the two mole fractions, $\tilde{Y}_{CO_2}$ and $\tilde{Y}_{H_2O}$, the soot volume fraction and the temperature, see relation (6). Thus, these results are required as an input for the radiation sources in the RTE. Note that these results showed a very good agreement with the experiment of [7], for details see Paul *et al.* [10].

The absorption coefficient, $\bar{\kappa}$, plotted in frame (e), shows that it is high in the region where the soot volume fraction as well as the temperature is large; clearly it is dominated by the soot volume fraction and the temperature rather than the mole fractions of CO_2 and H_2O, which proving the fact that the soot is the highly dominant element for the absorbing-emitting medium.

The results of the other radiation quantities are depicted in Fig. 4(f-j). The total radiative intensity, $\bar{I} = \sum_{m=1}^{M} \bar{I}_m$, shown in frame (f), is predicted maximum at the region where the high level of the absorption coefficient, $\bar{\kappa}$, was found. Similar pattern but different in magnitude is found for the incident radiation, $\bar{G}$, in frame (g), as this was obtained by summing over the total radiation multiplied by the weight factors in each direction. Moreover, the radiative heat flux vectors, $\bar{\mathbf{q}}$, presented in frame (h), show that the radiation transport is directed from the high sooting region, and their magnitudes further confirm that the radiative heat fluxes are dominated

by the soot volume fraction as well as the absorption coefficient. Furthermore, the divergence of the radiative heat flux, $\nabla.\bar{\mathbf{q}}$, in frame (j) shows clearly a massive amount of net energy gain due to the radiation in the highly sooting region.

5 Conclusions

The Discrete Ordinates Method (DOM/S_n) with the Large Eddy Simulation (LES) has been employed to investigate the radiative heat transfer of the luminous flame inside the three-dimensional cylindrical combustor. The absorption coefficient has been calculated as a function of the mole fractions of CO_2 and H_2O, the soot volume fraction ($\tilde{f}_v$) and the flame temperature; while the scattering was ignored in the present flame as it has been reported that the whole medium is dominated by the absorption.

The instantaneous results of the total radiation, incident radiation, radiative heat flux, and the divergence of heat flux have been obtained and presented in the paper. In the highly sooting region, where the absorption coefficient is large too, these results are predicted very high, which led to increase the net radiative energy. Various orders of approximation of S_n have been performed for the radiation modelling and it has been found that the results of the higher orders are in good agreement.

References

[1] C. R. Kaplan, S. W. Baek, E. S. Oran, J. L. Ellzey, Dynamics of a strongly radiating unsteady ethylene jet diffusion flame, Combustion and Flame 96 (1994) 1–21.

[2] P. E. Desjardin, S. H. Frankel, Two-dimentional large eddy simulation of soot formation in the near-field of strongly radiating nonpremixed acetylene-air turbulent jet flame, Combustion and Flame 119 (1999) 121–132.

[3] W. P. Jones, M. C. Paul, Combination of DOM with LES in a gas turbine combustor, Int. J. Eng. Science 43 (2005) 379–397.

[4] M. C. Paul, Performance of the various Sn approximations of DOM in a 3D combustion chamber, ASME J. Heat Transfer (2008) To appear in September.

[5] S. Chandrasekhar, Radiative Transfer, Dover Publications, 1960.

[6] B. G. Carlson, K. D. Lathrop, Transport Theory - The Method of Discrete Ordinates, Computing Methods in Reactor Physics (1968) 165–266.

[7] O. Nishida, S. Mukohara, Characteristics of soot formation and decomposition in turbulent diffusion flames, Combustion and Flame 47 (1982) 269–279.

[8] A. Leonard, Energy cascade in large-eddy simulations of turbulent fluid flows, Advances in Geophysics 18(A) (1974) 237–248.

[9] A. Favre, Statistical equations of turbulent cases in problems of hydrodynamics and continuum mechanics, Tech. rep., Society of Industrial and Applied Mathematics, Philadelphia (1969).

[10] S. C. Paul, M. C. Paul, W. P. Jones, LES for Soot Formation in a Propane-Air Turbulent Flame, Proceedings of the 5th Joint ASME/JSME Fluid Engineering Conference, San Diego, California, USA (2007).

[11] M. F. Modest, Radiative heat transfer, Academic Press, 2003.

[12] J. Smagorinsky, General circulation experiments with the primitive equations I. The basic experiment, Monthly Weather Review 91(3) (1963) 99–164.

[13] H. Schmidt, U. Schumann, Coherent structure of the convective boundary layer derived from large-eddy simulations, J. Fluid Mech. 200 (1989) 511–562.

[14] B. Zheng, C. X. Lin, M. A. Ebadian, Combined laminar forced convection and thermal radiation in a helical pipe, Int. J. Heat and Mass Transfer 43 (2000) 1067–1078.

[15] J. F. Thompson, F. C. Thames, C. W. Mastin, Automatic Numerical Generation of Body-Fitted Curvilinear Coordinate System for Field Containing Any Number of Arbitrary Two-Dimensional Bodies, J. Comp. Physics 15 (1974) 299–319.

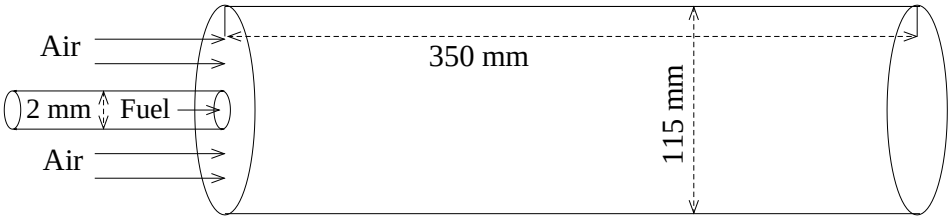

Figure 1: A schematic of the cylindrical combustion chamber.

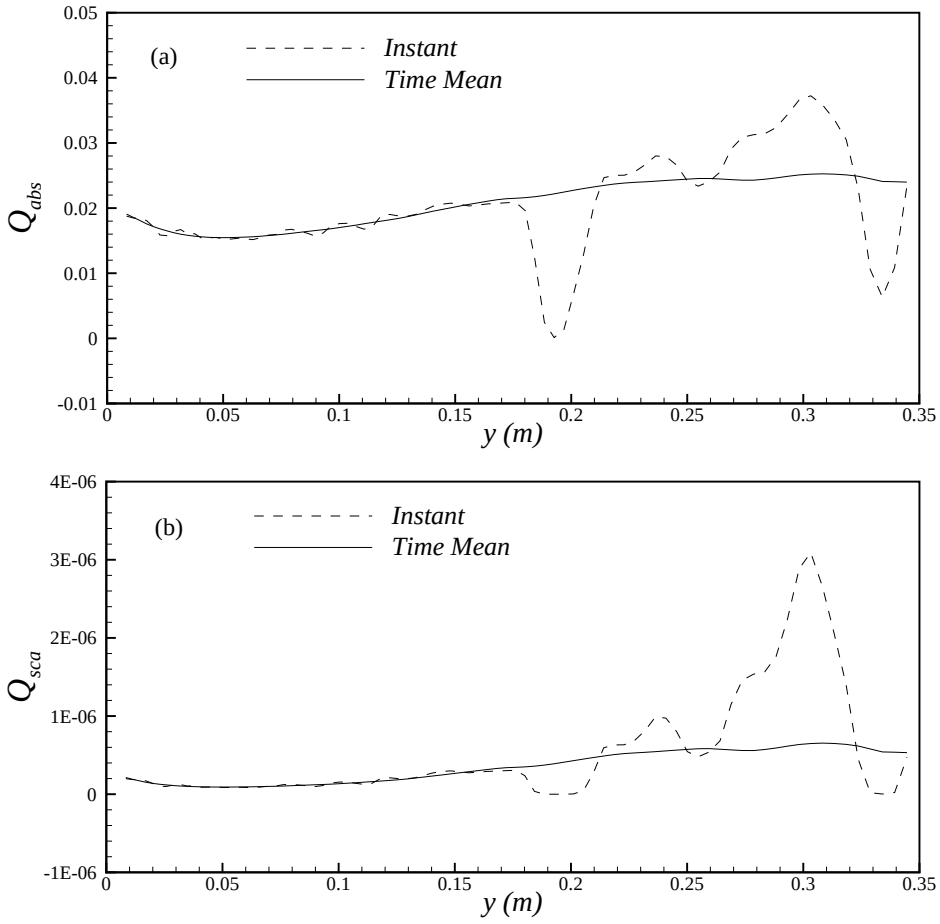

Figure 2: Axial plots of the (a) absorption and (b) scattering efficiencies.

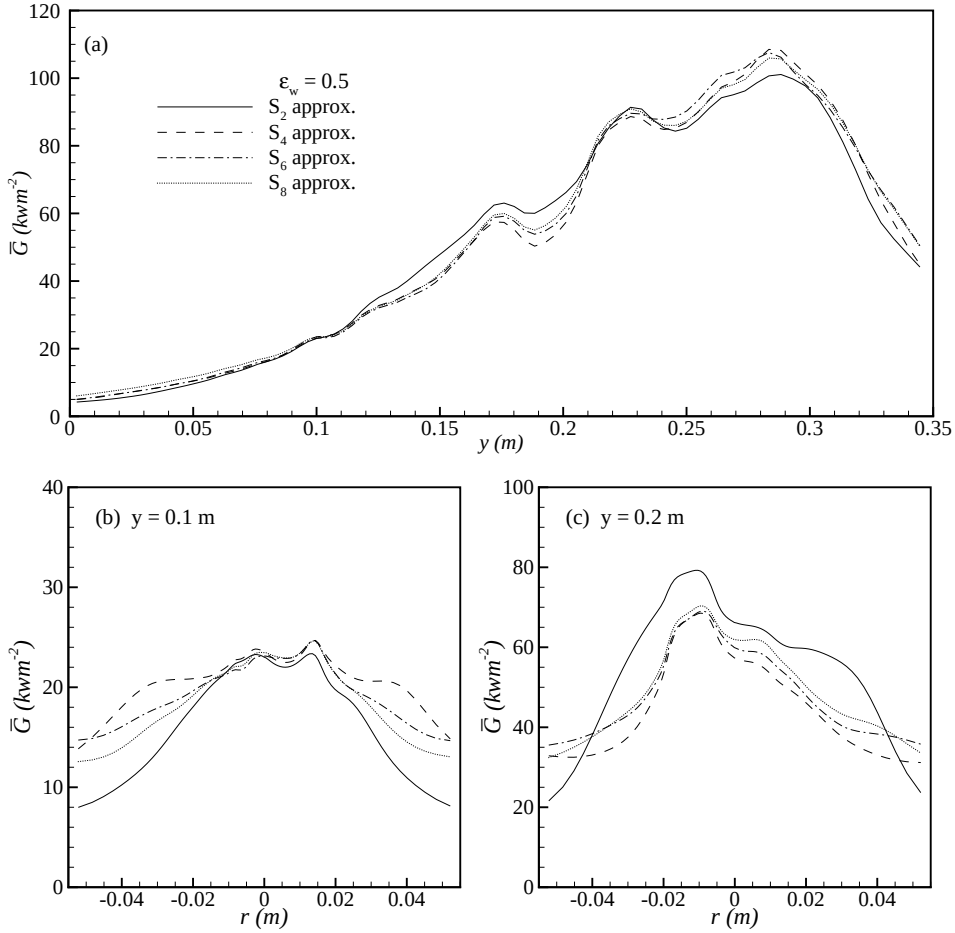

Figure 3: Incident radiation, $\bar{G}$ (kWm^{-2}), along (a) the axial direction, and the radial direction at (b) $y = 0.1m$, (c) $y = 0.2m$ and (d) $y = 0.3m$ for the different S_n approximations.

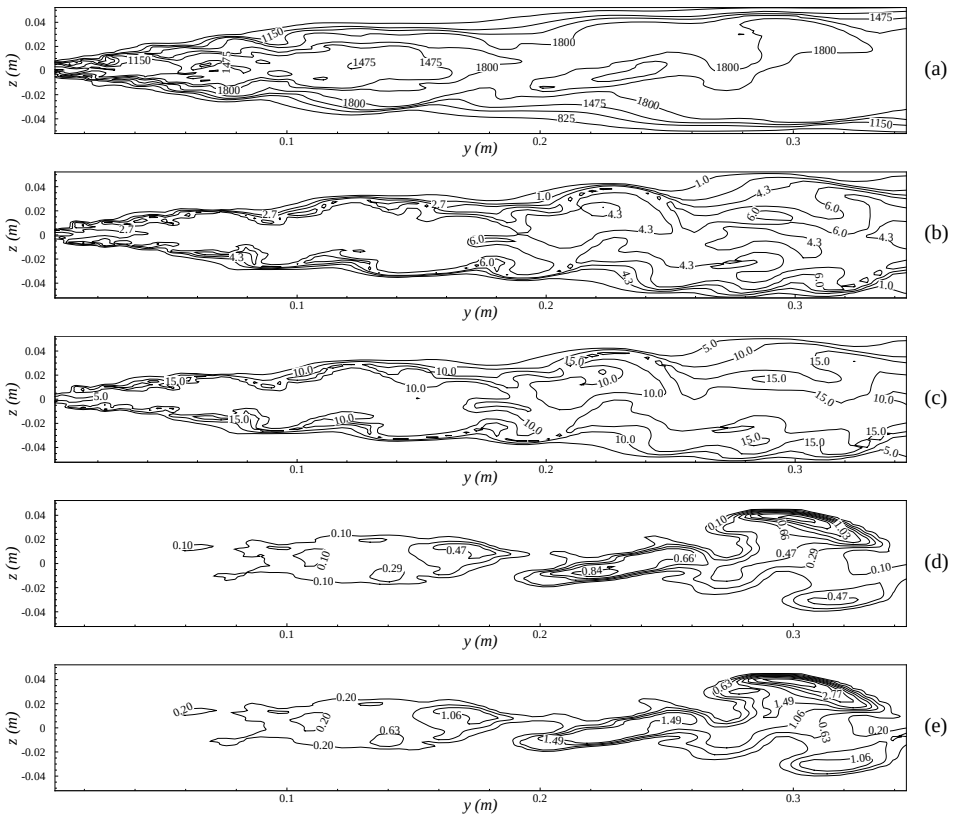

Figure 4: Instantaneous contour plots of (a) $\tilde{T}(K)$, (b) $\tilde{Y}_{CO_2} \times 10^{-2}$, (c) $\tilde{Y}_{H_2O} \times 10^{-2}$, (d) $\tilde{f}_v(ppm)$, (e) $\bar{\kappa}(m^{-1})$, (f) $\bar{I}(kWm^{-2})$, (g) $\bar{G}(kWm^{-2})$, (h) $\bar{\mathbf{q}}$, (i) $|\bar{\mathbf{q}}|(kWm^{-2})$ and (j) $\nabla.\bar{\mathbf{q}}(kWm^{-3})$ on the horizontal mid-plane of the combustor.

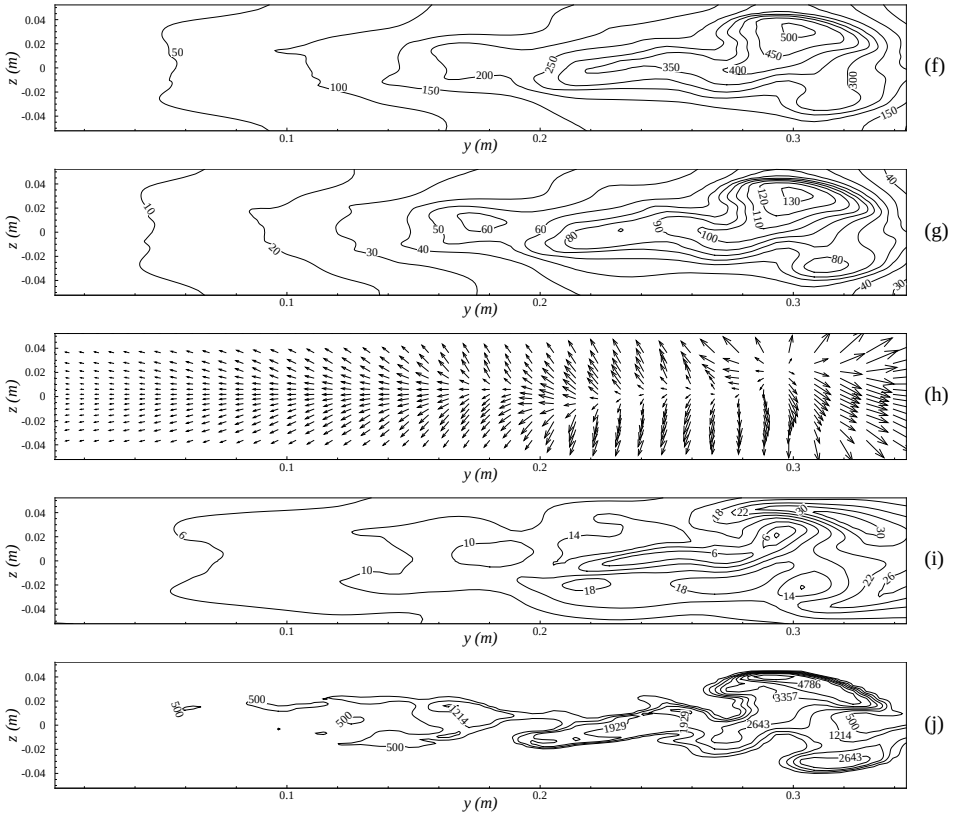

Figure 4: (continued)